TURUN
YLIOPISTO
UNIVERSITY
OF TURKU

FORMATION CONTROL OF SWARMS OF UNMANNED AERIAL VEHICLES

Anam Tahir

TURUN YLIOPISTON JULKAISUJA – ANNALES UNIVERSITATIS TURKUENSIS
SARJA – SER. F OSA – TOM. 27 | TECHNICA – INFORMATICA | TURKU 2023

TURUN
YLIOPISTO
UNIVERSITY
OF TURKU

FORMATION CONTROL OF SWARMS OF UNMANNED AERIAL VEHICLES

Anam Tahir

TURUN YLIOPISTON JULKAISUJA – ANNALES UNIVERSITATIS TURKUENSIS
SARJA – SER. F OSA – TOM. 27 | TECHNICA – INFORMATICA| TURKU 2023

University of Turku

Faculty of Technology
Department of Computing
Information and Communication Technology, Robotics and Autonomous Systems
Doctoral Programme in Technology

Supervised by

Professor Juha Plosila
University of Turku, Turku, Finland

Senior University Lecturer Jari Böling
Åbo Akademi University, Turku, Finland

Postdoctoral Researcher
Hashem Haghbayan
University of Turku, Turku, Finland

Reviewed by

Senior Lecturer Björn Olofsson
Lund University, Lund, Sweden

Senior Lecturer Jamshed Iqbal
University of Hull, Hull, United Kingdom

Opponent

Assistant Professor Azwirman Gusrialdi
Tampere University, Tampere, Finland

ISBN 978-951-29-9412-0 (PRINT)
ISBN 978-951-29-9411-3 (PDF)
ISSN 2736-9390 (PRINT)
ISSN 2736-9684 (ONLINE)
Painosalama Oy, Turku, Finland, 2023

Dedicated to my grandparents.

UNIVERSITY OF TURKU
Faculty of Technology
Department of Computing
Information and Communication Technology, Robotics and Autonomous Systems
TAHIR, ANAM: Formation Control of Swarms of
Unmanned Aerial Vehicles
Doctoral Dissertation, 85 pp.
Doctoral Programme in Technology
September 2023

ABSTRACT

The objective of this thesis is to design a distributed formation control system for swarms of unmanned aerial vehicles which addresses the challenges of scalability, collision avoidance, failure recovery, energy efficiency, and control performance. The swarms are arranged in tightly/loosely coupled architectures, which are based on homogeneous nodes in a distributed network of leader-follower/leaderless structures. The model of each node in the swarm formation is based on the nonlinear/linear dynamic model of a quadcopter, i.e. an unmanned aerial vehicle. The goal is to design the formation control of swarms of unmanned aerial vehicles, which is divided into high- and low-level control. From the high-level control perspective, the main contribution is to propose continuous path planning which can quickly react to events. Setpoints are generated for the swarms of unmanned aerial vehicles considering the complex movement of a hierarchical formation, soft landing, and failure recovery. The hierarchical formation and soft landing are executed using a fixed formation. Reconfiguration of the formation after node failures is implemented using a shortest path algorithm, combinatorial algorithms, and a thin plate spline. Besides this, from the low-level control perspective, the main contribution is to manoeuvre the nodes smoothly. The tracking of setpoints and stabilisation of each node is handled by a nonlinear sliding mode control with proportional derivative control and a linear quadratic regulator with integral action. The proposed strategies are evaluated using simulations, and the obtained results are compared and analysed both qualitatively and quantitatively using different scenario-relevant metrics.

KEYWORDS: Unmanned aerial vehicles, multi-drone systems, swarm intelligence, formation maintenance, distributed control, hierarchical systems, soft landing, failure recovery system.

TURUN YLIOPISTO
Teknillinen tiedekunta
Tietotekniikan laitos
Informaatio- ja viestintäteknologia, Robotiikka ja autonomiset järjestelmät
TAHIR, ANAM: Formation Control of Swarms of
Unmanned Aerial Vehicles
Väitöskirja, 85 s.
Teknologian tohtoriohjelma
Syyskuu 2023

TIIVISTELMÄ

Tämän opinnäytetyön tavoitteena on kehittää miehittämättömien ilma-alusten parville hajautettua muodostumisen ohjausta, joka vastaa skaalautuvuuden, törmäysten välttämisen, vikasietoisuuden, energiatehokkuuden ja ohjauksen suorituskyvyn haasteisiin. Parvet on järjestetty tiiviisti/löyhästi kytkettyihin arkkitehtuureihin, jotka perustuvat homogeenisiin yksikköihin hajautetussa johtaja-seuraaja-/johtajattomien rakenteiden verkostossa. Parvimuodostelman jokaisen yksikön malli perustuu nelikopterin eli miehittämättömän ilma-aluksen epälineaariseen dynaamiseen malliin. Tavoitteena on ehdottaa miehittämättömien ilma-alusten parvien muodostelmaohjausta, joka on jaettu korkean ja matalan tason ohjaukseen. Korkean tason ohjauksen näkökulmasta tärkein panos on ehdottaa jatkuvaa polun suunnittelua, joka pystyy reagoimaan nopeasti tapahtumiin. Asetusarvot luodaan miehittämättömien ilma-alusten parville ottaen huomioon hierarkkisen muodostelman monimutkaisen liikkeen, pehmeän laskun ja vikatilanteesta palautumisen. Hierarkkinen muodostelma ja pehmeä lasku suoritetaan kiinteällä muodostelmalla. Muodostelman uudelleenkonfigurointi yksiköiden vikatilanteiden jälkeen toteutetaan käyttämällä lyhimmän polun algoritmia, kombinatorisia algoritmeja ja ”thin plate spline” -algoritmia. Lisäksi matalan tason ohjauksen näkökulmasta tärkein panos on ohjata yksiköitä sujuvasti. Asetusarvojen seuranta ja kunkin yksikön stabilointi hoidetaan ”sliding mode” -säätimellä, jossa on suhde- ja derivoiva säätö, sekä lineaarisella neliösumman minimoivalla säätimellä, jossa on integroiva ominaisuus. Ehdotetut strategiat arvioidaan simuloinnilla, ja saatuja tuloksia verrataan ja analysoidaan sekä kvalitatiivisesti että kvantitatiivisesti käyttämällä erilaisia skenaarioihin liittyviä mittareita.

ASIASANAT: Miehittämättömät ilma-alukset, monidronejärjestelmät, parviälykkyys, muodostelman ylläpito, hajautettu ohjaus, hierarkkiset järjestelmät, pehmeä lasku, vikatilannetoipumusjärjestelmä.

Acknowledgements

I would like to express my deepest gratitude to my supervisors, Professor Juha Plosila, Senior University Lecturer Jari Böling, and Postdoctoral Researcher Hashem Haghbayan for their continued guidance, valuable support, and encouragement. Their patience and training in all aspects of being a good scientist are greatly appreciated and will not be forgotten. I am especially thankful to Senior University Lecturer Jari Böling for all the code/text reviews and continuous feedback, this thesis would not have been possible without his efforts. Furthermore, I am extremely grateful to my former supervisor Professor Hannu T. Toivonen, Åbo Akademi University, Turku, Finland, for his guidance on my studies.

I would like to thank University Lecturer Terho Jussila, Tampere University, Tampere, Finland, for suggesting, during my exchange programme, that I collaborate with Professor Hannu T. Toivonen, Åbo Akademi University, Turku, Finland, from where this journey began.

I would like to acknowledge my pre-examiners, Senior Lecturer Björn Olofsson and Senior Lecturer Jamshed Iqbal for providing constructive comments on the thesis. I extend special thanks to Assistant Professor Azwirman Gusrialdi for agreeing to be the opponent at the public thesis defence.

Many thanks to (i) University of Turku, Turku, Finland, (ii) ADAFI (Adaptive-Fidelity Digital Twins for Robust and Intelligent Control Systems); PI; Academy of Finland, project no. 335513, (iii) Finnish Cultural Foundation, Helsinki, Finland, decision no. 00211058, (iv) LARA (Learning and Assessing Risks for Enhancing Dependability of Autonomous Socio-Technical Systems); Co-PI; Academy of Finland, project no. 314048, (v) Turku University Foundation, Turku, Finland, and (vi) FinELib, National Library of Finland, Helsinki, Finland, for funding.

I would like to appreciate the people of the University of Turku, Turku, Finland, who were involved from time to time or provided moral support when needed on this long journey: Research Director Professor Hannu Tenhunen, Professor Tomi Westerlund, Researcher Jorge Peña Queralta, Laboratory Engineer Sami Nuuttila, Development Manager Marko Lahti, Coordinator Nina Lehtimäki, HR Specialist Nina Reini, Education Manager Sanna Ranto, Project Planning Officer Sonja Kareranta, Education Secretary Marja Luomanen, Vice Dean Professor Baoru Yang, and Facility Service Secretary Eveliina Jokinen. Also, I would like to thank Dr. Mahmood

Pervaiz, COMSATS University, Islamabad, Pakistan, and Principal Lecturer Eero Immonen, Turku University of Applied Sciences, Turku, Finland, for their guidance on my studies when needed. Furthermore, I would like to thank Aakkosto Oy for providing proofreading services.

Here, I would also like to acknowledge the support received from the people of the AMO and AT-IS Master's degree programmes of the Novia University of Applied Sciences, Finland, Valmet Automotive EV Power Oy, Finland, and Wärtsilä Finland Oy, with whom I got connected during the course of my doctoral degree.

I would like to close this with a few words for my family. My warmest gratitude goes to my parents, Dr. Tahir Sharif Malik and M.A. Ghazala Malik, and my sisters, Dr. Zona Tahir and Dr. Menahil Tahir, for all the love and support. Without their endless encouragement, I would be nowhere near where I am.

September 2023, Turku, Finland
Anam Tahir

ANAM TAHIR

Master of Engineering, Automation Technology – Intelligent Systems.
Novia University of Applied Sciences, Vaasa, Finland.

Master of Engineering, Autonomous Maritime Operations.
Novia University of Applied Sciences, Aboa Mare, Turku, Finland.

Master of Science, Electrical Engineering.
COMSATS University, Islamabad, Pakistan.

Bachelor of Science, Computer Engineering.
COMSATS University, Islamabad, Pakistan.

Table of Contents

Abbreviations

HLC	High-Level Control
LLC	Low-Level Control
LQR	Linear Quadratic Regulator
LTI	Linear Time-Invariant
PD	Proportional Derivative
SMC	Sliding Mode Control
TPS	Thin Plate Spline
UAV	Unmanned Aerial Vehicle
UGV	Unmanned Ground Vehicle
USV	Unmanned Surface Vehicle
UUV	Unmanned Underwater Vehicle
UV	Unmanned Vehicle

List of Original Publications

This thesis is based on the following original publications, which are referred to in the text by their Roman numerals:

I **Anam Tahir**, Jari Böling, Mohammad-Hashem Haghbayan, Hannu Toivonen, and Juha Plosila. Swarms of Unmanned Aerial Vehicles – A Survey. *Journal of Industrial Information Integration*, 2019; vol. 16 (100106): 1-7. DOI: https://doi.org/10.1016/j.jii.2019.100106

II **Anam Tahir**, Jari Böling, Mohammad-Hashem Haghbayan, and Juha Plosila. Comparison of Linear and Nonlinear Methods for Distributed Control of a Hierarchical Formation of UAVs. *IEEE Access*, 2020; vol. 8: 95667-95680. DOI: https://doi.org/10.1109/ACCESS.2020.2988773

III **Anam Tahir**, Jari Böling, Mohammad-Hashem Haghbayan, and Juha Plosila. Navigation System for Landing a Swarm of Autonomous Drones on a Movable Surface. *Communications of the ECMS, Proceedings of the 34th International ECMS Conference on Modelling and Simulation*, Wildau, Berlin, Germany, 2020; vol. 34, no. 1: 168–174. DOI: https://doi.org/10.7148/2020-0168

IV **Anam Tahir**, Jari Böling, Mohammad-Hashem Haghbayan, and Juha Plosila. Development of a Fault-Tolerant Control System for a Swarm of Drones. 62^{nd} *International Symposium ELMAR, IEEE Proceedings*, Zadar, Croatia, 2020; 79–82. DOI: https://doi.org/10.1109/ELMAR49956.2020.9219027

V **Anam Tahir**, Mohammad-Hashem Haghbayan, Jari Böling, and Juha Plosila. Energy-Efficient Post-Failure Reconfiguration of Swarms of Unmanned Aerial Vehicles. *IEEE Access*, 2023; vol. 11: 24768-24779. DOI: https://doi.org/10.1109/ACCESS.2022.3181244

1 Introduction

Swarms of unmanned vehicles (UVs) are sets of robots that work together to achieve a specific goal. They include vehicles moving on the ground, UGVs, in the air, UAVs, on the sea surface, USVs, or underwater, UUVs. UVs are increasingly getting attention on both recreational and military grounds[i] [1; 2; 3]. They can shape the future with the potential benefits of remote sensing and the elimination of human error. For example, UVs manoeuvre autonomously in and around and are capable of carrying out tasks in a variety of situational operations. Such vehicles can have innovative impacts in the areas of (a) security and surveillance, (b) data collection, (c) search and rescue, and (d) autonomous deliveries and shipping [4; 5; 6; 7].

UVs can operate in different modes depending upon their adaptation to versatile environmental conditions. The operational modes can be teleoperation, remote control, semi- or fully autonomous [8; 9].

- Teleoperation is a mode in which the human operator either directly controls the actuators or sets incremental objectives on a continuous basis, using sensory feedback from the location of the UVs [9].
- In comparison to the teleoperation mode, remote control is a mode in which the human operator controls the UVs on a continuous basis also from the location of the UVs but using only their direct observation [9]. In this mode, the UVs rely on input from the human operator.
- In contrast, a mode in which the UVs enjoy relative autonomy is the semi-autonomous mode. In this operational mode, an unmanned system and/or a human operator plan and conduct a mission that requires different levels of human interaction [9]. This enables the UVs to operate autonomously between human interactions.
- Going further, the fully autonomous mode is the mode of operation where the UVs have the most control without human intervention. It lets the UVs accomplish the assigned mission within the defined scope while adapting to operational and/or environmental conditions [9].

[i] UNMANNED AIRCRAFT SYSTEMS (UAS), DoD Purpose and Operational Use. Available at `https://dod.defense.gov/UAS/`, accessed on 09.06.2023.

In a formation based on distributed control, i.e., a bottom-up approach, a top-down approach is one of the main problems which lacks the perception of the overall dynamics of a swarm in a local controller of each UV. Hence, one of the important challenges in the formation of a swarm of UVs is the dependability of the swarm to proceed with its mission. As a solution, the purpose of this thesis is to address the distributed formation control problem, which enables dynamic management of the creation, maintenance, and termination of swarms with the challenges of scalability in terms of architecture. As a test case, unmanned aerial vehicles (UAVs) are considered, commonly known as drones. A detailed literature review of swarms of UAVs is presented in Publication I. To achieve better scalability, a methodology is proposed in which a high-level control (HLC) is integrated with a low-level control (LLC) so that the swarm performs the setpoint decision-making and an individual UAV tracks the given trajectory.

1.1 Preliminaries

The focus of this thesis is to explore multi-drone systems, i.e. swarms of UAVs, due to their vital challenges of formation control. It is defined as organising a set of nodes by maintaining its formation in a specific shape. To solve any formation control problem, three main components are considered i.e., system design, its modelling, and approaches of formation control structures [10; 11].

The system design delivers the framework upon which formation control is implemented such as:

- ***Homogeneity and Heterogeneity***
  Homogeneous nodes consist of similar modules of software and/or hardware whereas heterogeneous nodes consist of different software and/or hardware.

- ***Communication Structures***
  The communication structures of nodes can be listed with respect to their range, topology, and bandwidth.

- ***Centralised, Decentralised, and Distributed Networks***
  In the centralised network, as illustrated in Fig. 1(a), a single node acts as a server and holds all the information that is needed to obtain the desired objectives. Hence, these networks are prone to hacks and failures as it takes only one node to be compromised or shut down for the entire network to collapse. On the other hand, decentralised and distributed networks do not rely on a central node, as described in Fig. 1(b)-(c). These networks provide greater user control, system dependability, scalability, and privacy. Decentralised and distributed networks have several characteristics and they are not synonymous. Decentralised networks make use of a range of distinct con-

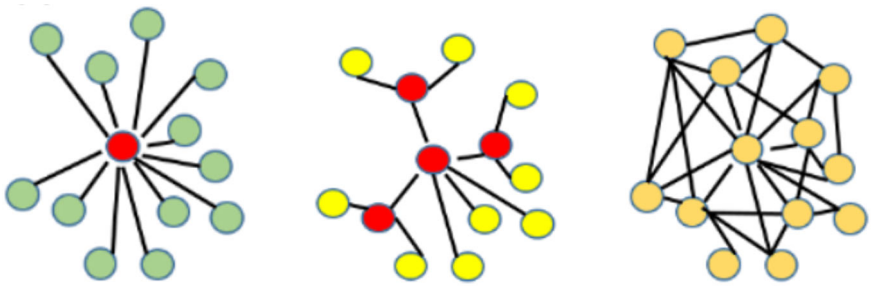

(a) Centralised (b) Decentralised (c) Distributed

Figure 1. Network formations [12].

necting nodes. In decentralised networks, each node can have independent decision-making and information processing. The functionality is distributed across the network, which prevents total system failures or breakdowns. In contrast, distributed networks behave in a transparent manner, for example, location data is shared and decision-making is divided between the nodes, which is absent in decentralised networks. Hence, their distinguishing characteristic is reliance on equally powerful connecting hubs. However, unlike decentralised networks, these can become centralised, and can also refer to dispersed networks with a top-down approach. As a result, troubleshooting is easier as the system failures, incursions, and crashes may be traced back to specific nodes, making it easier to pinpoint the source of the problem. In addition, hybrid centralised/decentralised/distributed networks, in turn, use central planners to provide HLC over autonomous robots.

The modelling of UAVs is based on their mathematical models, discussed in Chapter 2. Furthermore, a formation structure defines how a group of UAVs can be controlled to form and maintain the desired formation. To control the formation of swarms, the recent literature normally classifies the different structures into the following main categories [13], as presented in Fig. 2.

- ***Leader-follower [14; 15; 16; 17]***
  A leader aims for team objectives, while the follower(s) track the paths of the leader with prescribed offsets. This structure is prone to error propagation and sensitive to the leader's failure.

- ***Virtual [18; 19; 20]***
  Letting each node have its own trajectory will solve the error propagation but cannot avoid collisions.

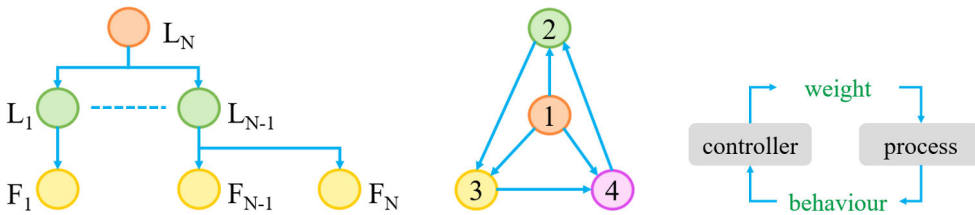

(a) Leader-follower (b) Virtual (c) Behaviour-based

Figure 2. Formation structures.

- ***Behaviour-based [21; 22; 23]***
  To form the desired shape of a swarm, each node is assigned to one of the several desired behaviours. The overall control is then derived from a weighting of the relative importance of each behaviour. This structure is scalable, but cannot ensure a fixed pattern.

The formation structures can be further categorised into position, displacement, distance, and angle based with regards to the need for interaction topology and sensing capability [24]. The formation in position-based control is defined by the desired positions of nodes with respect to the global coordinate system. Also, it is assumed that each node can sense its own position. In contrast to this, the formation in displacement-based control is defined by the desired displacements between pairs of nodes with respect to the global coordinate system. Also, each node can sense its own and its neighbour node(s)' positions, which ensures maintaining the same orientation. Furthermore, the formation in distance-based control is defined by the desired inter-node distances that are actively controlled. Besides this, in angle-based control, the actively controlled variable is the bearing between neighbours. In distance- or angle-based control, distance assignment instead of position assignment is present for pairs of nodes. The controlled variables are also the distances to the sensed neighbours or the bearings between pairs of neighbours. Hence, all the variables can be sensed locally as there is no need for a global or aligned coordinate system.

1.2 Problem Formulation

Inspired by the aforementioned discussions, the first key element that needs to be adapted in most swarms of UAVs is scalability so that a swarm can be further divided into subgroups. One of the main problems in distributed formation control of swarms of UAVs is enabling the dynamic management of the creation, maintenance, and termination of swarms. The following questions are addressed in this thesis:

1 ***System design for swarms of UAVs***
What different set-ups are used for formation control of swarms of UAVs, and which set-up should be used in this study?

2 ***High-level control (HLC)***
How to design a control system which can handle hierarchical formation, soft landing, and failure recovery while maintaining its formation with collision avoidance? This procedure is defined as the mapping problem, which describes the best shape of the desired swarm formations.

3 ***Low-level control (LLC)***
How do UAVs smoothly manoeuvre in the formations, arranged in tightly and loosely coupled architectures? This problem addresses the optimal tracking movement of each node from its initial to final position in a swarm formation.

1.3 Thesis Layout

This thesis is divided into five chapters. The introduction and the problem formulation are stated in Chapter 1. The models of UAVs are outlined in Chapter 2. The methodology for designing formation control of swarms of UAVs is elaborated in Chapter 3. The concluding remarks are discussed in Chapter 4. Lastly, the overview of publications is presented in Chapter 5.

In a swarm formation, most of the state-of-the-art is focused on the distributed controllers i.e., the local controller of each UAV. It only manipulates its actuators based on the observations of the local dynamic model of each node i.e., a bottom-up approach. Hence, it is unaware of the behaviour and constraints of the swarm's higher levels of hierarchy i.e., the top-down approach. Both approaches try to refine and optimise the partial behaviour of the systems, which eventually leads to global emergent behaviour. This optimal or near-optimal behaviour of the system is the final goal of control designs. This work addresses the problem of a distributed formation control that is based on the dynamics of the overall swarm and the local dynamics of each node via implementing the partial controllers i.e., the top-down, bottom-up approach.

As a preliminary study, a comprehensive literature review of the general research field of UAVs, with a particular emphasis on swarms is presented in Publication I. In addition, an online survey among the general public was performed to investigate the public awareness of the technology field. The model of each node in the swarm formation is based on the nonlinear (Publications II, IV, and V) and linear (Publication III) dynamic models of a quadcopter, i.e. a UAV. This work is based on the formation control of swarms of homogeneous UAVs in a distributed network of leader-follower and leaderless structures in Publications II-IV and Publication V respectively. It sheds light on the challenges of scalability, collision avoidance, fail-

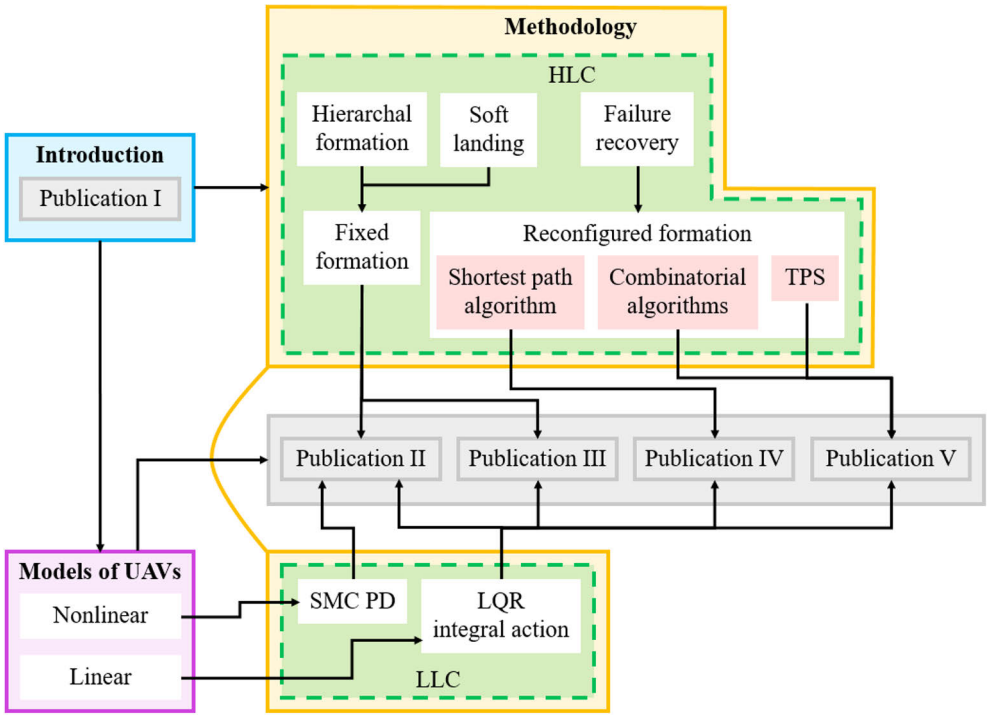

Figure 3. Structure of the thesis.

ure recovery, energy efficiency, and control performance. This addresses Research Question 1. The goal is to design the formation control of swarms of UAVs, which is divided into HLC and LLC, as explained in Fig.3.

In the HLC, to avoid collisions among UAVs, setpoints are generated for the swarms of UAVs considering the complex movement of a hierarchical formation, soft landing, and failure recovery. The hierarchical formation and soft landing are executed using a fixed formation in Publications II and III respectively. The reconfiguration of the formation after a single failed node is implemented using a shortest path algorithm in Publication IV. For multiple failed nodes, the reconfiguration of the formation is implemented using combinatorial algorithms (i.e., distance- and time-optimal algorithms) and thin plate spline (TPS) method in Publication V. This addresses Research Question 2.

Besides this, in the LLC, the tracking of setpoints and stabilisation of each node for smooth manoeuvre is handled by a nonlinear sliding mode control (SMC) with proportional derivative (PD) control in Publication II and a linear quadratic regulator (LQR) with integral action in Publications II-V. This addresses Research Question 3.

2 Models of Unmanned Aerial Vehicles

The model of each node in the swarm formation consists of the nonlinear (Publications II, IV, and V) and linear (Publication III) dynamic models of a quadcopter, i.e. UAV. Exhibiting the concept of the proposed control designs, this model presents itself as a case study for swarms of UAVs.

Each UAV in a swarm is responsible for tracking the desired trajectories as well as for hovering at desired positions for given time periods. In this section, the dynamic model of a quadcopter is examined. Consider a quadcopter as shown in Fig. 4(a), commonly known as a drone, an under-actuated system having four input engines and propellers enabling six degrees of freedom including roll ϕ, pitch θ, yaw ψ, and thrust for movement and manoeuvre. For most quadcopter designs, there are two possible configurations as illustrated in Fig. 4(b), i.e. plus and cross [25; 26; 27]. In each configuration, the two rotors on the opposite ends always rotate in the same direction while the other two rotate in the opposite direction, whereas all the thrusts have the same direction.

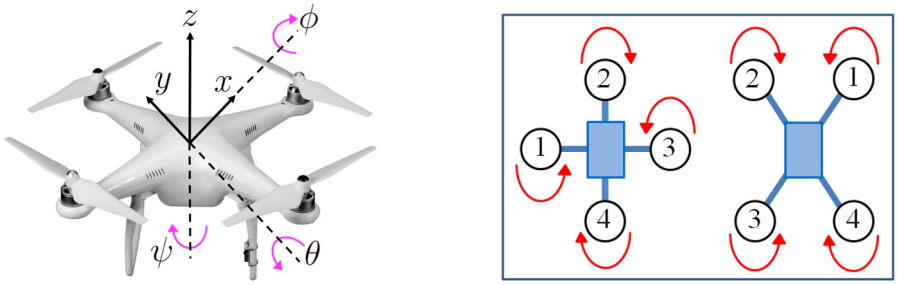

(a) (b)

Figure 4. (a) Quadcopter's movement about the axis. (b) Configuration of a quadcopter.

The direction of movement, i.e. rotations, is the roll ϕ, pitch θ, and yaw ψ, which are affected by thrusts from the propeller. The roll ϕ, pitch θ, and yaw ψ movements are controlled to ensure the stability of rotation around the x-axis (longitudinal axis), y-axis (lateral or transverse axis), and z-axis (vertical axis) respectively. In other words, the roll ϕ is the measure of side-to-side tilting, i.e., it causes the vehicle to move to one side or the other depending on the tilt. The pitch θ determines the

rotation of the vehicle fixed between the side-to-side axis, i.e., it would tilt the vehicle up and down from front to back causing the vehicle to move forwards or backward depending on which way it is tilted. The yaw ψ moves the vehicle around in a clockwise/anticlockwise rotation as it stays level to the ground, i.e., it changes the direction of the vehicle accordingly. However, the thrust is not a directional element like roll ϕ, pitch θ, and yaw ψ, but controls the altitude of the vehicle.

2.1 Nonlinear Model

Consider a quadcopter that has four propellers with fixed pitch mechanically movable blades, as described in Fig. 5.

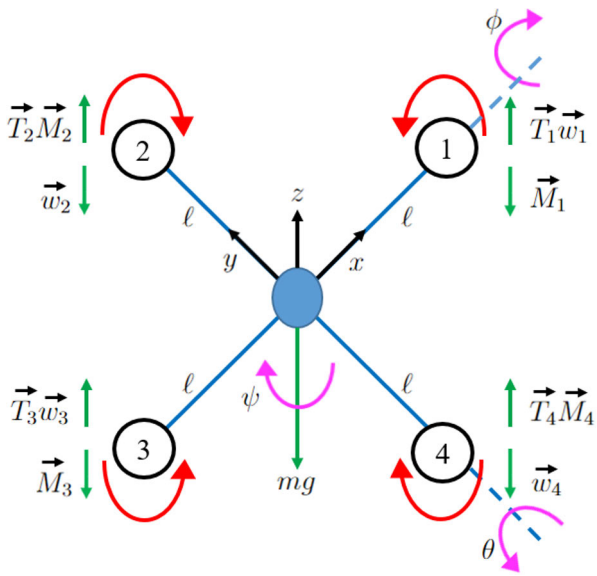

Figure 5. Kinematics of the quadcopter.

The major forces acting on the quadcopter are the gravity g and the thrust T_i, $i \in \{1, 2, 3, 4\}$, of the propellers. In this model, the inertial reference is the earth shown as (x, y, z) which is the origin of the reference frame. A quadcopter is assumed to be a rigid body that has a constant mass symmetrically distributed with respect to the planes (x, y), (y, z), and (x, z).

The position of a quadcopter reference frame (x, y, z) with respect to an inertial frame $(x, y, z)_0$ can be expressed mathematically in a state variable form [28; 29] where translational and angular accelerations are given by

$$\begin{aligned}\dot{v}_x &= -v_z w_y + v_y w_z - g\sin\theta \\ \dot{v}_y &= -v_x w_z + v_z w_x + g\cos\theta\sin\phi \\ \dot{v}_z &= -v_y w_x + v_x w_y + g\cos\theta\cos\phi - \frac{T}{m}\end{aligned} \tag{1}$$

and

$$\begin{aligned}\dot{w}_x &= \frac{1}{J_x}(-w_y w_z(J_z - J_y) + M_x - \frac{k_{wT}}{k_{MT}} J_{mp} M_z w_y) \\ \dot{w}_y &= \frac{1}{J_y}(-w_x w_z(J_x - J_z) + M_y - \frac{k_{wT}}{k_{MT}} J_{mp} M_z w_x) \\ \dot{w}_z &= \frac{M_z}{J_z}\end{aligned} \tag{2}$$

respectively. The thrust produced by each propeller T_i is translated into a total thrust T and the reactive torques M_i, $i \in \{x, y, z\}$, affecting the rotations along the corresponding axis. J_i, $i \in \{x, y, z\}$, is known as the moment of inertia along the corresponding axis, and J_{mp} is the moment of inertia of a motor with a propeller. The angular velocities of propellers are assumed to be proportional to the thrusts of propellers i.e., $w_j = k_{wT} T_i$, $j \in \{x, y, z\}$. Similarly, the reactive moments of propellers are assumed to be proportional to the thrust of propellers i.e., $M_i = k_{MT} T_i$. Depending on the chosen configuration, the propeller thrusts T_i will generate different thrust T and torques M_i namely

$$\begin{bmatrix} T \\ M_x \\ M_y \\ M_z \end{bmatrix} = \begin{bmatrix} 1 & 1 & 1 & 1 \\ 0 & -\ell & 0 & \ell \\ \ell & 0 & -\ell & 0 \\ k_{MT} & -k_{MT} & k_{MT} & -k_{MT} \end{bmatrix} \begin{bmatrix} T_1 \\ T_2 \\ T_3 \\ T_4 \end{bmatrix} \tag{3}$$

for a plus configuration and

$$\begin{bmatrix} T \\ M_x \\ M_y \\ M_z \end{bmatrix} = \begin{bmatrix} 1 & 1 & 1 & 1 \\ \frac{\sqrt{2}}{2}\ell & -\frac{\sqrt{2}}{2}\ell & -\frac{\sqrt{2}}{2}\ell & \frac{\sqrt{2}}{2}\ell \\ \frac{\sqrt{2}}{2}\ell & \frac{\sqrt{2}}{2}\ell & -\frac{\sqrt{2}}{2}\ell & -\frac{\sqrt{2}}{2}\ell \\ k_{MT} & -k_{MT} & k_{MT} & -k_{MT} \end{bmatrix} \begin{bmatrix} T_1 \\ T_2 \\ T_3 \\ T_4 \end{bmatrix} \tag{4}$$

for a cross configuration where ℓ is the length of the fixed pitch to mechanically movable blades [30]. The velocities corresponding to Equations (1) and (2) are

$$\begin{aligned}
\dot{x} &= v_x \cos\psi \cos\theta + v_y(-\sin\psi \cos\phi + \cos\psi \sin\theta \sin\phi) + \\
&\quad v_z(\sin\psi \sin\phi + \cos\psi \sin\theta \cos\phi) \\
\dot{y} &= v_x \sin\psi \cos\theta + v_y(\cos\psi \cos\phi + \sin\psi \sin\theta \sin\phi) + \\
&\quad v_z(-\cos\psi \sin\phi + \sin\psi \sin\theta \cos\phi) \\
\dot{z} &= v_x \sin\theta - v_y \cos\theta \sin\phi - v_z \cos\theta \cos\phi
\end{aligned} \tag{5}$$

and

$$\begin{aligned}
\dot{\theta} &= w_y \cos\phi - w_z \sin\phi \\
\dot{\phi} &= w_x + w_y \sin\phi \tan\theta + w_z \cos\phi \tan\theta \\
\dot{\psi} &= w_y \frac{\sin\phi}{\cos\theta} + w_z \frac{\cos\phi}{\cos\theta}
\end{aligned} \tag{6}$$

respectively. Equations (1) to (6) represent the complete nonlinear model of a quadcopter, composed of twelve states, four inputs, and twelve outputs. More precisely,

$$\mathbf{x} = \begin{bmatrix} v_x & v_y & v_z & w_x & w_y & w_z & \theta & \phi & \psi & x & y & z \end{bmatrix}^{\mathrm{T}} \tag{7}$$

is the state or system vector,

$$\mathbf{u} = \begin{bmatrix} T & M_x & M_y & M_z \end{bmatrix}^{\mathrm{T}} \tag{8}$$

is the input or control vector, and

$$\mathbf{y} = \mathbf{x} \tag{9}$$

is the output (measured) vector. In any practical setting, some of the states would be estimated using numerical derivation or integration with respect to time. The nonlinear equations can be expressed in a compact form

$$\dot{\mathbf{x}} = f(x, u). \tag{10}$$

Furthermore, the reduced state vector

$$\mathbf{x_s} = \begin{bmatrix} v_x & v_y & v_z & w_x & w_y & w_z \end{bmatrix}^{\mathrm{T}} \tag{11}$$

and the performance outputs

$$y_{p_1} \in \{x, y, z\}, \tag{12}$$

$$y_{p_2} \in \{\theta, \phi, \psi\}, \tag{13}$$

and

$$\mathbf{y_p} = \begin{bmatrix} x & y & z \end{bmatrix}^{\mathrm{T}} \tag{14}$$

are defined for future use. $\{v_x, v_y, v_z\}$ and $\{w_x, w_y, w_z\}$ are defined as translational and angular velocities respectively. Furthermore, y_{p_1} and y_{p_2} are defined as the translational and angular positions respectively. The values assigned to each quadcopter are illustrated in Table 1, which are used in analytical solutions and simulations.

Table 1. System parameters [28].

Symbol	Quantity	Value
g	gravitational force	9.81 m/s^2
ℓ	length of the blades	0.2 m
m	mass of the quadcopter	0.8 kg
J_{mp}	moment of inertia of motor with propeller	$\approx 0^*$
J_x, J_y	moment of inertia with respect to axis (x, y)	1.8×10^{-3} kgm^2
J_z	moment of inertia with respect to axis z	1.5×10^{-3} kgm^2
k_{MT}	ratio of reactive moment and thrust of used propellers	0.1 m

* Assuming zero means that the rpm of a propeller can be directly manipulated.

2.2 Linear Model

In reconnaissance missions, the prevailing state of a quadcopter is either to have a slow flight or to hover in equilibrium with all the state derivatives equal to zero such as $\dot{\mathbf{x}} = 0$, known as an equilibrium point. Putting all the derivatives to zero in nonlinear Equations (1) to (6) leads to equilibrium values,

$$\begin{aligned} T_0 &= mg \quad \text{and} \\ M_{x_0} &= M_{y_0} = M_{z_0} = 0, \end{aligned} \tag{15}$$

for the manipulated variables.

Consequently, nonlinear dynamic equations can be converted into standard equations of a linear system by assuming small values of state variables and small differences of manipulated variables from equilibrium using a standard linearisation method given by

$$\dot{\mathbf{x}} = \mathbf{A}\mathbf{x} + \mathbf{B}\mathbf{u} \tag{16}$$

where $\mathbf{A} = [A_{ij}]$ and $\mathbf{B} = [B_{ij}]$, defined as

$$A_{ij} = \frac{\partial f_i}{\partial x_j} | x = x_0, u = u_0 \tag{17}$$

and

$$B_{ij} = \frac{\partial f_i}{\partial u_j}|x = x_0, u = u_0, \tag{18}$$

are the matrices with functions as constant elements for the state vector $\mathbf{x}$ from Equation (7) and the input or control vector $\mathbf{u}$ from Equation (8) respectively. The matrices' components are established systemically term by term at the equilibrium point $(x_0, u_0) = (0, 0)$.

Consider Equation (10) and Equation (16) where $\mathbf{x}$ does not depend on $\mathbf{u}$ so the derivative with respect to $\mathbf{u} = 0$. Differentiating $f_1 = -v_z w_y + v_y w_z - g \sin\theta$ with respect to $\mathbf{x}$ leads to

$$\begin{aligned}
&\frac{\partial f_1}{\partial x_2} = \frac{\partial f_1}{\partial v_y} = w_z|_0 = 0,\\
&\frac{\partial f_1}{\partial x_3} = \frac{\partial f_1}{\partial v_z} = -w_y|_0 = 0,\\
&\frac{\partial f_1}{\partial x_5} = \frac{\partial f_1}{\partial w_y} = -v_z|_0 = 0,\\
&\frac{\partial f_1}{\partial x_6} = \frac{\partial f_1}{\partial w_z} = v_y|_0 = 0, \text{ and}\\
&\frac{\partial f_1}{\partial x_7} = \frac{\partial f_1}{\partial \theta} = -g\cos\theta|_0 = -g.
\end{aligned} \tag{19}$$

Differentiating $f_2 = -v_x w_z + v_z w_x + g\cos\theta\sin\phi$ with respect to $\mathbf{x}$ leads to

$$\begin{aligned}
&\frac{\partial f_2}{\partial x_1} = \frac{\partial f_2}{\partial v_x} = -w_z|_0 = 0,\\
&\frac{\partial f_2}{\partial x_3} = \frac{\partial f_2}{\partial v_z} = w_x|_0 = 0,\\
&\frac{\partial f_2}{\partial x_4} = \frac{\partial f_2}{\partial w_x} = v_z|_0 = 0,\\
&\frac{\partial f_2}{\partial x_6} = \frac{\partial f_2}{\partial w_z} = -v_x|_0 = 0,\\
&\frac{\partial f_2}{\partial x_7} = \frac{\partial f_2}{\partial \theta} = -g\sin\theta\sin\phi|_0 = 0, \text{ and}\\
&\frac{\partial f_2}{\partial x_8} = \frac{\partial f_2}{\partial \phi} = g\cos\theta\cos\phi|_0 = g.
\end{aligned} \tag{20}$$

Differentiating $f_3 = -v_y w_x + v_x w_y + g\cos\theta\cos\phi$ with respect to $\mathbf{x}$ leads to

$$\begin{aligned}
\frac{\partial f_3}{\partial x_1} &= \frac{\partial f_3}{\partial v_x} = w_y|_0 = 0, \\
\frac{\partial f_3}{\partial x_2} &= \frac{\partial f_3}{\partial v_y} = -w_x|_0 = 0, \\
\frac{\partial f_3}{\partial x_4} &= \frac{\partial f_3}{\partial w_x} = -v_y|_0 = 0, \\
\frac{\partial f_3}{\partial x_5} &= \frac{\partial f_3}{\partial w_y} = v_x|_0 = 0, \\
\frac{\partial f_3}{\partial x_7} &= \frac{\partial f_3}{\partial \theta} = -g\sin\theta\cos\phi|_0 = 0, \text{ and} \\
\frac{\partial f_3}{\partial x_8} &= \frac{\partial f_3}{\partial \phi} = -g\cos\theta\sin\phi|_0 = 0.
\end{aligned} \tag{21}$$

Differentiating $f_4 = \frac{1}{J_x}(-w_y w_z(J_z - J_y))$ with respect to $\mathbf{x}$ leads to

$$\begin{aligned}
\frac{\partial f_4}{\partial x_5} &= \frac{\partial f_4}{\partial w_y} = \frac{-w_z(J_z - J_y)}{J_x}|_0 = 0 \quad \text{and} \\
\frac{\partial f_4}{\partial x_6} &= \frac{\partial f_4}{\partial w_z} = \frac{-w_y(J_z - J_y)}{J_x}|_0 = 0.
\end{aligned} \tag{22}$$

Differentiating $f_5 = \frac{1}{J_y}(-w_x w_z(J_x - J_z))$ with respect to $\mathbf{x}$ leads to

$$\begin{aligned}
\frac{\partial f_5}{\partial x_4} &= \frac{\partial f_5}{\partial w_x} = \frac{-w_z(J_x - J_z)}{J_y}|_0 = 0 \quad \text{and} \\
\frac{\partial f_5}{\partial x_6} &= \frac{\partial f_5}{\partial w_z} = \frac{-w_x(J_x - J_z)}{J_y}|_0 = 0.
\end{aligned} \tag{23}$$

Differentiating $f_6 = 0$ with respect to $\mathbf{x}$ leads to 0. Differentiating $f_7 = w_y\cos\phi - w_z\sin\phi$ with respect to $\mathbf{x}$ leads to

$$\begin{aligned}
\frac{\partial f_7}{\partial x_5} &= \frac{\partial f_7}{\partial w_y} = \cos\phi|_0 = 1, \\
\frac{\partial f_7}{\partial x_6} &= \frac{\partial f_7}{\partial w_z} = -\sin\phi|_0 = 0, \text{ and} \\
\frac{\partial f_7}{\partial x_8} &= \frac{\partial f_7}{\partial \phi} = (-w_y\sin\phi - w_z\cos\phi)|_0 = 0.
\end{aligned} \tag{24}$$

Differentiating $f_8 = w_x + w_y\sin\phi\tan\theta + w_z\cos\phi\tan\theta$ with respect to $\mathbf{x}$ leads to

$$\begin{aligned}
\frac{\partial f_8}{\partial x_4} &= \frac{\partial f_8}{\partial w_x} = 1, \\
\frac{\partial f_8}{\partial x_5} &= \frac{\partial f_8}{\partial w_y} = \sin\phi \tan\theta|_0 = 0, \\
\frac{\partial f_8}{\partial x_6} &= \frac{\partial f_8}{\partial w_z} = \cos\phi \tan\theta|_0 = 0, \\
\frac{\partial f_8}{\partial x_7} &= \frac{\partial f_8}{\partial \theta} = (w_y \sin\phi \sec^2\theta + w_z \cos\phi \sec^2\theta)|_0 = 0, \text{ and} \\
\frac{\partial f_8}{\partial x_8} &= \frac{\partial f_8}{\partial \phi} = (w_y \cos\phi \tan\theta - w_z \sin\phi \tan\theta)|_0 = 0.
\end{aligned} \tag{25}$$

Differentiating $f_9 = w_y \frac{\sin\phi}{\cos\theta} + w_z \frac{\cos\phi}{\cos\theta}$ with respect to $\mathbf{x}$ leads to

$$\begin{aligned}
\frac{\partial f_9}{\partial x_5} &= \frac{\partial f_9}{\partial w_y} = \frac{\sin\phi}{\cos\theta}|_0 = 0, \\
\frac{\partial f_9}{\partial x_6} &= \frac{\partial f_9}{\partial w_z} = \frac{\cos\phi}{\cos\theta}|_0 = 1, \\
\frac{\partial f_9}{\partial x_7} &= \frac{\partial f_9}{\partial \theta} = (w_y \sin\phi(\frac{-1}{\sqrt{1-\theta^2}}) + w_z \cos\phi(\frac{-1}{\sqrt{1-\theta^2}}))|_0 = 0, \text{ and} \\
\frac{\partial f_9}{\partial x_8} &= \frac{\partial f_9}{\partial \phi} = (w_y \frac{\cos\phi}{\cos\theta} - w_z \frac{\sin\phi}{\cos\theta})|_0 = 0.
\end{aligned} \tag{26}$$

Differentiating $f_{10} = v_x \cos\psi\cos\theta + v_y(-\sin\psi\cos\phi + \cos\psi\sin\theta\sin\phi) + v_z(\sin\psi\sin\phi + \cos\psi\sin\theta\cos\phi)$ with respect to $\mathbf{x}$ leads to

$$\begin{aligned}
\frac{\partial f_{10}}{\partial x_1} &= \frac{\partial f_{10}}{\partial v_x} = \cos\psi\cos\theta|_0 = 1, \\
\frac{\partial f_{10}}{\partial x_2} &= \frac{\partial f_{10}}{\partial v_y} = (-\sin\psi\cos\phi + \cos\psi\sin\theta\sin\phi)|_0 = 0, \\
\frac{\partial f_{10}}{\partial x_3} &= \frac{\partial f_{10}}{\partial v_z} = (\sin\psi\sin\phi + \cos\psi\sin\theta\cos\phi)|_0 = 0, \\
\frac{\partial f_{10}}{\partial x_7} &= \frac{\partial f_{10}}{\partial \theta} = (-v_x\cos\psi\sin\theta + v_y\cos\psi\cos\theta\sin\phi + \\
&\quad v_z\cos\psi\cos\theta\cos\phi)|_0 = 0, \\
\frac{\partial f_{10}}{\partial x_8} &= \frac{\partial f_{10}}{\partial \phi} = (v_y\sin\psi\sin\phi + v_y\cos\psi\sin\theta\cos\phi + v_z\sin\psi\cos\phi - \\
&\quad v_z\cos\psi\sin\theta\sin\phi)|_0 = 0, \text{ and} \\
\frac{\partial f_{10}}{\partial x_9} &= \frac{\partial f_{10}}{\partial \psi} = (-v_x\sin\psi\cos\theta - v_y\cos\psi\cos\phi - v_y\sin\psi\sin\theta\sin\phi + \\
&\quad v_z\cos\psi\sin\phi - v_z\sin\psi\sin\theta\cos\phi)|_0 = 0.
\end{aligned} \tag{27}$$

Differentiating $f_{11} = v_x \sin\psi\cos\theta + v_y(\cos\psi\cos\phi + \sin\psi\sin\theta\sin\phi) + v_z(-\cos\psi\sin\phi + \sin\psi\sin\theta\cos\phi)$ with respect to $\mathbf{x}$ leads to

$$\begin{aligned}
&\frac{\partial f_{11}}{\partial x_1} = \frac{\partial f_{11}}{\partial v_x} = \sin\psi\cos\theta|_0 = 0,\\
&\frac{\partial f_{11}}{\partial x_2} = \frac{\partial f_{11}}{\partial v_y} = (\cos\psi\cos\phi + \sin\psi\sin\theta\sin\phi)|_0 = 1,\\
&\frac{\partial f_{11}}{\partial x_3} = \frac{\partial f_{11}}{\partial v_z} = (-\cos\psi\sin\phi + \sin\psi\sin\theta\cos\phi)|_0 = 0,\\
&\frac{\partial f_{11}}{\partial x_7} = \frac{\partial f_{11}}{\partial \theta} = (-v_x\sin\psi\sin\theta + v_y\sin\psi\cos\theta\sin\phi +\\
&\quad v_z\sin\psi\cos\theta\cos\phi)|_0 = 0,\\
&\frac{\partial f_{11}}{\partial x_8} = \frac{\partial f_{11}}{\partial \phi} = (-v_y\cos\psi\sin\phi + v_y\sin\psi\sin\theta\cos\phi - v_z\cos\psi\cos\phi -\\
&\quad v_z\sin\psi\sin\theta\sin\phi)|_0 = 0, \text{ and}\\
&\frac{\partial f_{11}}{\partial x_9} = \frac{\partial f_{11}}{\partial \psi} = (v_x\cos\psi\cos\theta - v_y\sin\psi\cos\phi + v_y\cos\psi\sin\theta\sin\phi +\\
&\quad v_z\sin\psi\sin\phi + v_z\cos\psi\sin\theta\cos\phi)|_0 = 0.
\end{aligned} \tag{28}$$

Differentiating $f_{12} = v_x\sin\theta - v_y\cos\theta\sin\phi - v_z\cos\theta\cos\phi$ with respect to $\mathbf{x}$ leads to

$$\begin{aligned}
&\frac{\partial f_{12}}{\partial x_1} = \frac{\partial f_{12}}{\partial v_x} = \sin\theta|_0 = 0,\\
&\frac{\partial f_{12}}{\partial x_2} = \frac{\partial f_{12}}{\partial v_y} = -\cos\theta\sin\phi|_0 = 0,\\
&\frac{\partial f_{12}}{\partial x_3} = \frac{\partial f_{12}}{\partial v_z} = -\cos\theta\cos\phi|_0 = -1,\\
&\frac{\partial f_{12}}{\partial x_7} = \frac{\partial f_{12}}{\partial \theta} = (v_x\cos\theta + v_y\sin\theta\sin\phi + v_z\sin\theta\cos\phi)|_0 = 0, \text{ and}\\
&\frac{\partial f_{12}}{\partial x_8} = \frac{\partial f_{12}}{\partial \phi} = (-v_y\cos\theta\cos\phi + v_z\cos\theta\sin\phi)|_0 = 0.
\end{aligned} \tag{29}$$

Keeping all the attained differential values from Equations (19) to (29) into Equation (17), the matrix

$$A_{ij} = \begin{bmatrix} 0 & 0 & 0 & 0 & 0 & 0 & -g & 0 & 0 & 0 & 0 & 0 \\ 0 & 0 & 0 & 0 & 0 & 0 & 0 & g & 0 & 0 & 0 & 0 \\ 0 & 0 & 0 & 0 & 0 & 0 & 0 & 0 & 0 & 0 & 0 & 0 \\ 0 & 0 & 0 & 0 & 0 & 0 & 0 & 0 & 0 & 0 & 0 & 0 \\ 0 & 0 & 0 & 0 & 0 & 0 & 0 & 0 & 0 & 0 & 0 & 0 \\ 0 & 0 & 0 & 0 & 0 & 0 & 0 & 0 & 0 & 0 & 0 & 0 \\ 0 & 0 & 0 & 0 & 1 & 0 & 0 & 0 & 0 & 0 & 0 & 0 \\ 0 & 0 & 0 & 1 & 0 & 0 & 0 & 0 & 0 & 0 & 0 & 0 \\ 0 & 0 & 0 & 0 & 0 & 1 & 0 & 0 & 0 & 0 & 0 & 0 \\ 1 & 0 & 0 & 0 & 0 & 0 & 0 & 0 & 0 & 0 & 0 & 0 \\ 0 & 1 & 0 & 0 & 0 & 0 & 0 & 0 & 0 & 0 & 0 & 0 \\ 0 & 0 & -1 & 0 & 0 & 0 & 0 & 0 & 0 & 0 & 0 & 0 \end{bmatrix} \tag{30}$$

with functions as constant elements is obtained for the state vector $\mathbf{x}$.

Consider Equation (10) and Equation (16) where $\mathbf{u}$ does not depend on $\mathbf{x}$ so the derivative with respect to $\mathbf{x} = 0$. Differentiating $f_1 = -\frac{T}{m}$ with respect to $\mathbf{u}$ leads to

$$\frac{\partial f_1}{\partial u_1} = \frac{\partial f_1}{\partial T} = -\frac{1}{m}|_0 = -\frac{1}{m}. \tag{31}$$

Differentiating $f_2 = \frac{M_x}{J_x}$ (where $J_{mp} = 0$, see Table 1) with respect to $\mathbf{u}$ leads to

$$\frac{\partial f_2}{\partial u_2} = \frac{\partial f_2}{\partial M_x} = \frac{1}{J_x}|_0 = \frac{1}{J_x}. \tag{32}$$

Differentiating $f_3 = \frac{M_y}{J_y}$ (where $J_{mp} = 0$, see Table 1) with respect to $\mathbf{u}$ leads to

$$\frac{\partial f_3}{\partial u_3} = \frac{\partial f_3}{\partial M_y} = \frac{1}{J_y}|_0 = \frac{1}{J_y}. \tag{33}$$

Differentiating $f_4 = \frac{M_z}{J_z}$ with respect to $\mathbf{u}$ leads to

$$\frac{\partial f_4}{\partial u_4} = \frac{\partial f_4}{\partial M_z} = \frac{1}{J_z}|_0 = \frac{1}{J_z}. \tag{34}$$

Keeping all the attained differential values from Equations (31) to (34) into Equation (18), the matrix

$$B_{ij} = \begin{bmatrix} 0 & 0 & -\frac{1}{m} & 0 & 0 & 0 & 0 & 0 & 0 & 0 & 0 & 0 \\ 0 & 0 & 0 & \frac{1}{J_x} & 0 & 0 & 0 & 0 & 0 & 0 & 0 & 0 \\ 0 & 0 & 0 & 0 & \frac{1}{J_y} & 0 & 0 & 0 & 0 & 0 & 0 & 0 \\ 0 & 0 & 0 & 0 & 0 & \frac{1}{J_z} & 0 & 0 & 0 & 0 & 0 & 0 \end{bmatrix}^{\mathrm{T}} \tag{35}$$

with functions as constant elements is obtained for the input or control vector $\mathbf{u}$.

Hence, the complete dynamics of a quadcopter can be represented in a standard linear time-invariant (LTI) form

$$\dot{\mathbf{x}} = \begin{bmatrix} 0&0&0&0&0&0&-g&0&0&0&0&0 \\ 0&0&0&0&0&0&0&g&0&0&0&0 \\ 0&0&0&0&0&0&0&0&0&0&0&0 \\ 0&0&0&0&0&0&0&0&0&0&0&0 \\ 0&0&0&0&0&0&0&0&0&0&0&0 \\ 0&0&0&0&0&0&0&0&0&0&0&0 \\ 0&0&0&0&1&0&0&0&0&0&0&0 \\ 0&0&0&1&0&0&0&0&0&0&0&0 \\ 0&0&0&0&0&1&0&0&0&0&0&0 \\ 1&0&0&0&0&0&0&0&0&0&0&0 \\ 0&1&0&0&0&0&0&0&0&0&0&0 \\ 0&0&-1&0&0&0&0&0&0&0&0&0 \end{bmatrix} \begin{bmatrix} v_x \\ v_y \\ v_z \\ w_x \\ w_y \\ w_z \\ \theta \\ \phi \\ \psi \\ x \\ y \\ z \end{bmatrix} + \begin{bmatrix} 0&0&0&0 \\ 0&0&0&0 \\ -\frac{1}{m}&0&0&0 \\ 0&\frac{1}{J_x}&0&0 \\ 0&0&\frac{1}{J_y}&0 \\ 0&0&0&\frac{1}{J_z} \\ 0&0&0&0 \\ 0&0&0&0 \\ 0&0&0&0 \\ 0&0&0&0 \\ 0&0&0&0 \\ 0&0&0&0 \end{bmatrix} \begin{bmatrix} 0 \\ 0 \\ T \\ M_x \\ M_y \\ M_z \\ 0 \\ 0 \\ 0 \\ 0 \\ 0 \\ 0 \end{bmatrix} \tag{36}$$

using Equations (16), (30) and (35). More precisely, it can be written as

$$\begin{aligned} \dot{\mathbf{x}} &= \mathbf{A}\mathbf{x} + \mathbf{B}\mathbf{u} \\ &= \begin{bmatrix} -g\theta & g\phi & -\frac{T}{m} & \frac{M_x}{J_x} & \frac{M_y}{J_y} & \frac{M_z}{J_z} & w_y & w_x & w_z & v_x & v_y & -v_z \end{bmatrix}^{\mathrm{T}} \end{aligned} \tag{37}$$

and

$$\mathbf{y} = \mathbf{C}\mathbf{x} + \mathbf{D}\mathbf{u} = \mathbf{x} \tag{38}$$

where $\mathbf{C}$ and $\mathbf{D}$ are defined as output (measured) matrix and feedthrough matrix respectively. The state or system vector, input or control vector, output (measured) vector, reduced state vector, and the performance outputs are given in Equations (7) to (9) and (11) to (14) respectively.

3 Methodology

In this thesis, the model of each node in the swarm formation is based on the nonlinear (Publications II, IV, and V) and linear (Publication III) dynamic models of a quadcopter, i.e. a UAV. The goal is to design the formation control of swarms of UAVs, which is divided into HLC and LLC, as presented in Fig.3. The HLC(s) relies on continuous monitoring, which communicates with the LLC(s), as explained in Fig. 6. In particular, the HLC integrates a continuous path planning and execution cycle which can quickly react to events. In contrast, the LLC decides the control modes and the associated trajectories taking into account the mission, path, and control constraints and requirements of each UAV in a swarm.

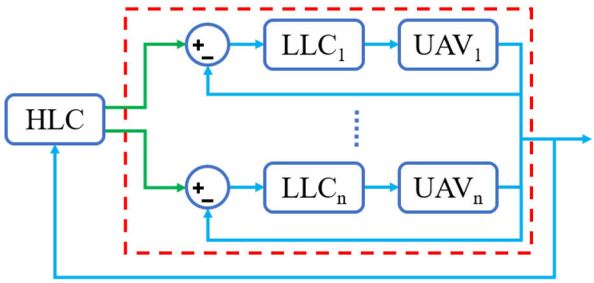

Figure 6. Overall control scheme.

3.1 High-Level Control

In the HLC, the setpoints are generated using offsets in Publication II to maintain the hierarchical formation of UAVs in the swarms. In contrast, the setpoints are generated using offsets in Publication III to guarantee the smoothness, i.e. soft landing, of desired landing missions on a movable surface while minimising the possibilities for landing errors. The hierarchical formation and soft landing are executed using a fixed formation. Besides this, the failure recovery method is included, which reconfigures the swarm formation after single and multiple failed nodes in Publications IV and V respectively. For reconfigurations, the setpoints are generated using the shortest path algorithm in Publication IV. In contrast, the setpoints are generated using combinatorial algorithms (i.e., distance- and time-optimal algorithms) and the TPS method in Publication V. Only the TPS method is described in the following subsection.

3.1.1 Thin Plate Spline

For robust nonrigid 2D transformation, consider a point set registration [31; 32; 33] using TPS, which is known for solving data interpolation and smoothing problems [34]. A spline is a function defined by polynomials in a piecewise manner. For the approximation of complicated shapes, spline curves are used via curve fitting that is adaptable and has noncomplicated construction [34]. To make it simpler, this method is analysed in 2D in Publication V. Consequently, two sets of correspondence data points, $X = x_i$ and $V = v_i$ where $i = 1, 2, 3, ..., n$ are considered. Here, x_i and v_i are defined as the locations of a point in the desired formation (scene) and the initial formation (model) respectively. Keeping the shape of the disturbed formation/function under consideration, a mapping function $f(v_i)$ can be obtained by minimising the energy function

$$E_{TPS}(f) = \sum_{i=1}^{n} ||x_i - f(v_i)||^2 + \lambda \iint \big((\frac{\partial^2 f}{\partial x^2})^2 + 2(\frac{\partial^2 f}{\partial x \partial y})^2 + (\frac{\partial^2 f}{\partial y^2})\big) dxdy \quad (39)$$

that evaluates the amount of formation disturbance. The data points of V are mapped as closely as possible to the data points of X by minimising the first error measurement term. The second regularisation term is a penalty on the smoothness of f, and it is in a general case needed to make the mapping unique. In the cases that are studied in this thesis, one can put $\lambda = 0$, and still get unique solutions.

3.2 Low-Level Control

In the LLC, a feedback controller is designed to track the setpoints and stabilise the positions of UAVs for smooth manoeuvre in a swarm formation. The tracking of setpoints and stabilisation of each UAV is handled by LQR with integral action in Publications II-V and SMC PD in Publication II. This is further described in the following subsections.

3.2.1 Linear Quadratic Regulator with Integral Action

LQR is a simple control design method that provides good control performance in the full-state feedback case and can handle a multivariable system [35]. For the formation flight, a standard LQR augmented with integral action is tested as illustrated in Fig. 7, similar to what was done in [36] and [37]. Each UAV has its local control system, with the setpoints coming from the above level. LQR provides an optimal full-state feedback controller using linear model Equations (37) and (38), which is tested on the nonlinear model Equations (1) to (6) of each UAV in Publications II, IV, and V whereas it is tested on the linear model Equations (37) and (38) of each UAV in Publication III.

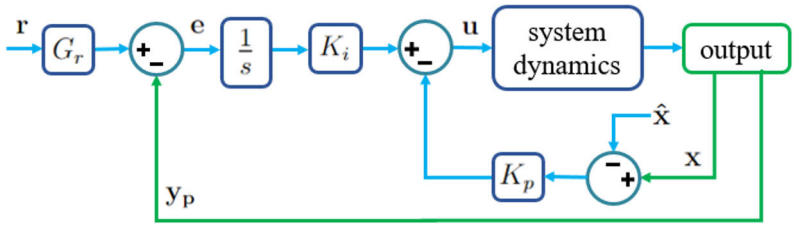

Figure 7. Block diagram of LQR integral control design.

Considering the linear model Equations (37) and (38), the control input $\mathbf{u}$ minimises the quadratic cost function

$$J(\mathbf{u}) = \int_0^\infty (\dot{\mathbf{x}}_\mathbf{a}^\mathrm{T} Q \dot{\mathbf{x}}_\mathbf{a} + \dot{\mathbf{u}}^\mathrm{T} R \dot{\mathbf{u}}) dt \tag{40}$$

where

$$\mathbf{x_a} = \begin{bmatrix} \int_0^t \mathbf{e}(\tau)^\mathrm{T}\, d\tau & \mathbf{x}^\mathrm{T} \end{bmatrix}^\mathrm{T}, \tag{41}$$

the states $\mathbf{x}$, and the control vector $\mathbf{u}$ are defined in Equations (7) and (8) respectively. Q is a positive semi-definite matrix that defines the weights of states, whereas R is a positive definite matrix that weights the control inputs. To get the desired response, the controller can be tuned by changing the (diagonal) elements in the Q and R matrices. Positive-definite and semi-definite criteria for the diagonal matrices mean that the diagonal elements are greater than zero and greater than or equal to zero respectively. A larger diagonal element in Q or R means fewer variations in the corresponding state or control input respectively. Furthermore,

$$\mathbf{e} = \mathbf{r} - \mathbf{y_p} \tag{42}$$

is the error term and

$$\mathbf{r} = \begin{bmatrix} x_r & y_r & z_r \end{bmatrix}^\mathrm{T} \tag{43}$$

is the reference for $\mathbf{y_p}$, defined in Equation (14). The state feedback law

$$\mathbf{u} = \frac{K_i}{s}\mathbf{e} - K_p(\mathbf{x} - \hat{\mathbf{x}}) \tag{44}$$

gives the four control inputs i.e., thrust T and torques M_i; M_x (along x-axis i.e. roll ϕ), M_y (along y-axis i.e. pitch θ), and M_z (along z-axis i.e. yaw ψ). The controller uses two separate gain matrices K_p and K_i where K_p is the state feedback gain and K_i is the integral gain. $\hat{\mathbf{x}}$ is the setpoints of the states $\mathbf{x}$ and G_r is the reference gain.

3.2.2 Sliding Mode Control with Proportional Derivative Control

The SMC method reduces the order of the state equations and provides a quick response, which leads to the simplification of a design procedure. It may reduce the system's sensitivity with respect to parameter variation and disturbances when it enters the sliding surface. However, this may lead to a chattering phenomenon that can be minimised by using proper switching gains in the saturation function. Furthermore, PD control is a closed-loop system in which the proportional controller reduces the rise time and steady-state error, and the derivative controller reduces overshoot, increases the stability of the system, and improves the transient response.

For the formation flight, an SMC PD control method from [38] is adapted and tested on the nonlinear model Equations (1) to (6) of each UAV in Publication II. Fig. 8 shows the control design of each UAV, which is divided into two feedback control loops, i.e., outer and inner, where $\mathbf{x_s}$, y_{p_1}, and y_{p_2} are defined in Equations (11) to (13). Furthermore,

$$r_1 \in \{x_r, y_r, z_r\} \tag{45}$$

is the reference for y_{p_1}. In this control design, SMC is tied to the PD control and the gain parameters can be adjusted based on the overall dynamics of the swarm, which eventually produces input or control vector $\mathbf{u}$, defined in Equation (8). A UAV's translational position y_{p_1} is handled by the outer feedback control loop using PD control whereas angular position is handled by the inner feedback control loop using SMC. This is further described in the following subsections.

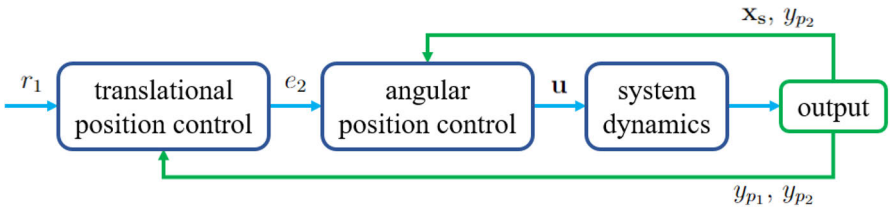

Figure 8. Block diagram of SMC PD control design.

Translational Position Control Design

The control design of each UAV's translational positions y_{p_1} is described in Fig. 9. Using three PD controllers, the angular position errors $e_2 \in \{\theta_e, \phi_e, \psi_e\}$ are generated, which are fed to the angular position control design as inputs. The feedback law

$$e_2 = y_{p_2} - r_2 = y_{p_2} - (K_P \cdot e_1 + K_D \frac{d}{dt} e_1) \tag{46}$$

is obtained where $e_1 = r_1 - y_{p_1}$, and the parameters K_P and K_D are the proportional and derivative gains respectively. y_{p1} and y_{p2} are the translational and angular positions respectively, see Equations (12) and (13).

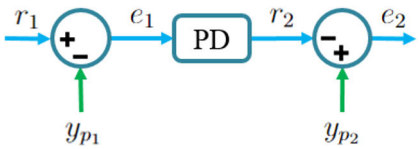

Figure 9. The translational position control design.

Furthermore, to control the hierarchical formation of tightly coupled architectures, a lead compensator is connected in series with the PD control block, which reduces the overshoots of translational positions y_{p_1}. Mathematically, the transfer function

$$G(s) = \frac{s - z_z}{s - z_p} \tag{47}$$

is defined as the lead compensator where z_z is the zero and z_p is the pole, satisfying $0 < z_z < z_p$.

Angular Position Control Design

For each UAV, the input or control vector $\mathbf{u}$, see Equation (8), is obtained using four SMC controllers. The actuator thrust T is generated to drive each UAV, and the torques $M_i \in \{M_x, M_y, M_z\}$ are generated for the stabilisation of the position angles, as presented in Fig. 10.

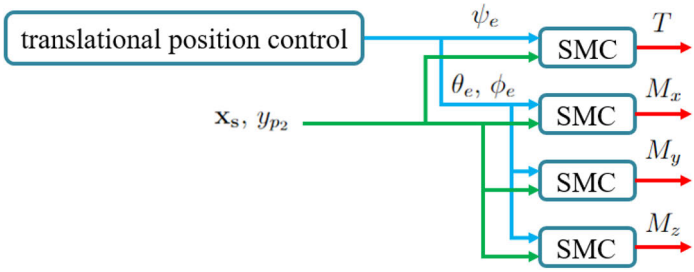

Figure 10. The angular position control design.

Consider a time-varying surface $s_a(t)$ in the state space $\mathbb{R}^n$ by the scalar equation $s_a(x,t) = 0$. The sliding surface

$$s_\alpha = c_\alpha e_\alpha + \dot{e}_\alpha \tag{48}$$

is chosen where $\alpha \in \{T, M_x, M_y, M_z\}$, c_α is a strictly positive constant, and e_α is the tracking error [39]. The chattering free control law

$$\alpha = \hat{\alpha} - K_\alpha \text{sat}(\frac{s_\alpha}{\beta_\alpha}) \tag{49}$$

for thrust T and torques M_i; M_x (along x-axis i.e. roll ϕ), M_y (along y-axis i.e. pitch θ), and M_z (along z-axis i.e. yaw ψ) is obtained. The control design parameters $\hat{\alpha}$, defined as equivalent control, and K_α indicate the motion of the state trajectory along the sliding surface s_α and the maximum controller output respectively. To eliminate the chattering phenomena, the saturation function

$$\text{sat}(\frac{s_\alpha}{\beta_\alpha}) = \begin{cases} \frac{s_\alpha}{\beta_\alpha}, & |\frac{s_\alpha}{\beta_\alpha}| \leq 1 \\ \text{sgn}(\frac{s_\alpha}{\beta_\alpha}), & \text{otherwise} \end{cases} \tag{50}$$

allocates a low pass filter to the local dynamics of the variable s_α, which approximates the sgn(.) term in a boundary layer of the manifold $s_a(t) = 0$. This boundary layer solution avoids control discontinuities and switching actions in the control loop. The β_α is a constant that defines the thickness of the boundary layer. The control design is more efficient when a minimum amount of boundary layer is used. The method of obtaining the equivalent control $\hat{\alpha}$ is described below.

Differentiating the Equation (48) with respect to e leads to

$$\dot{s}_\alpha = c_\alpha \dot{e}_\alpha + \ddot{e}_\alpha \tag{51}$$

for thrust T and torques M_i. The sliding surfaces

$$\begin{aligned} \dot{s}_T &= c_T \dot{z} + \ddot{z}, \\ \dot{s}_{M_x} &= c_{M_x} \dot{\phi} + \ddot{\phi}, \\ \dot{s}_{M_y} &= c_{M_y} \dot{\theta} + \ddot{\theta}, \text{ and} \\ \dot{s}_{M_z} &= c_{M_z} \dot{\psi} + \ddot{\psi} \end{aligned} \tag{52}$$

are obtained by letting $\{\dot{e}_T, \dot{e}_{M_x}, \dot{e}_{M_y}, \dot{e}_{M_z}\} = \{\dot{z}, \dot{\phi}, \dot{\theta}, \dot{\psi}\}$ respectively. Keeping the $\dot{z}$ from Equation (5) and $\dot{v}_z$ from Equation (1) in Equation (52),

$$\begin{aligned} \dot{s}_T &= c_T(v_x \sin\theta - v_y \cos\theta \sin\phi - v_z \cos\theta \cos\phi) + \frac{d}{dz}\dot{z} \\ &= c_T(v_x \sin\theta - v_y \cos\theta \sin\phi - v_z \cos\theta \cos\phi) - \dot{v}_z \cos\theta \cos\phi \\ &= c_T(v_x \sin\theta - v_y \cos\theta \sin\phi - v_z \cos\theta \cos\phi) - \\ &(-v_y w_x + v_x w_y + g \cos\theta \cos\phi - \frac{T}{m}) \cos\theta \cos\phi \end{aligned} \tag{53}$$

is obtained for the thrust T. Keeping the $\dot{\phi}$ from Equation (6) and $\dot{w}_x$ from Equation (2) where $J_{mp} = 0$, see Table 1, in Equation (52),

$$\begin{aligned}\dot{s}_{Mx} &= c_{Mx}(w_x + w_y \sin\phi \tan\theta + w_z \cos\phi \tan\theta) + \frac{d}{dx}\dot{\phi} \\ &= c_{Mx}(w_x + w_y \sin\phi \tan\theta + w_z \cos\phi \tan\theta) + \dot{w}_x \\ &= c_{Mx}(w_x + w_y \sin\phi \tan\theta + w_z \cos\phi \tan\theta) + \\ &\frac{1}{J_x}(-w_y w_z (J_z - J_y) + M_x)\end{aligned} \tag{54}$$

is obtained for the torque M_x. Keeping the $\dot{\theta}$ from Equation (6) and $\dot{w}_y$ from Equation (2) where $J_{mp} = 0$, see Table 1, in Equation (52),

$$\begin{aligned}\dot{s}_{My} &= c_{My}(w_y \cos\phi - w_z \sin\phi) + \frac{d}{dy}\dot{\theta} \\ &= c_{My}(w_y \cos\phi - w_z \sin\phi) + \dot{w}_y \cos\phi \\ &= c_{My}(w_y \cos\phi - w_z \sin\phi) + (\frac{1}{J_y}(-w_x w_z (J_x - J_z) + M_y)) \cos\phi\end{aligned} \tag{55}$$

is obtained for the torque M_y. Keeping the $\dot{\psi}$ from Equation (6) and $\dot{w}_z$ from Equation (2) in Equation (52),

$$\begin{aligned}\dot{s}_{Mz} &= c_{Mz}(w_y \frac{\sin\phi}{\cos\theta} + w_z \frac{\cos\phi}{\cos\theta}) + \frac{d}{dz}\dot{\psi} \\ &= c_{Mz}(w_y \frac{\sin\phi}{\cos\theta} + w_z \frac{\cos\phi}{\cos\theta}) + \dot{w}_z \frac{\cos\phi}{\cos\theta} \\ &= c_{Mz}(w_y \frac{\sin\phi}{\cos\theta} + w_z \frac{\cos\phi}{\cos\theta}) + \frac{M_z}{J_z}\frac{\cos\phi}{\cos\theta}\end{aligned} \tag{56}$$

is obtained for the torque M_z. Let $\{\dot{s}_T, \dot{s}_{Mx}, \dot{s}_{My}, \dot{s}_{Mz}\} = 0$ in Equations (53) to (56), the equivalent control $\hat{\alpha}$;

$$\begin{aligned}\hat{T} &= -\frac{mc_T}{\cos\theta\cos\phi}(v_x \sin\theta - v_y \cos\theta \sin\phi - v_z \cos\theta \cos\phi) + \\ &\quad m(-v_y w_x + v_x w_y + g\cos\theta\cos\phi), \\ \hat{M}_x &= -c_{Mx} J_x (w_x + w_y \sin\phi \tan\theta + w_z \cos\phi \tan\theta) + w_y w_z (J_z - J_y), \\ \hat{M}_y &= -\frac{c_{My} J_y}{\cos\phi}(w_y \cos\phi - w_z \sin\phi) + w_x w_z (J_x - J_z), \text{ and} \\ \hat{M}_z &= -c_{Mz} J_z (w_y \tan\phi + w_z)\end{aligned} \tag{57}$$

is obtained for the Equation (49).

The control law α from Equation (49) ensures both the reachability condition $s_\alpha \dot{s}_\alpha < 0$ and the sliding condition $\dot{V}_\alpha = \frac{1}{2}\frac{d}{dt}s_\alpha^2$ using Lyapunov's stability analysis, given below. Consider a positive definite scalar function for the thrust T and torques M_i as

$$V_\alpha = \frac{1}{2}s_\alpha^2 \tag{58}$$

and its derivative leads to

$$\dot{V}_\alpha = s_\alpha \dot{s}_\alpha \tag{59}$$

where $\dot{s}_\alpha$ is given in Equations (53) to (56). Keeping the control law α from Equation (49) and the equivalent control $\hat{\alpha}$ from Equation (57) in Equation (59),

$$\dot{V}_\alpha = -\eta|s_\alpha| < 0 \tag{60}$$

is obtained by letting K_α;

$$\begin{aligned} K_T &= \frac{m}{\cos\theta\cos\phi}, \\ K_{M_x} &= J_x, \\ K_{M_y} &= \frac{J_y}{\cos\phi}, \text{ and} \\ K_{M_z} &= \frac{J_z\cos\theta}{\cos\phi}, \end{aligned} \tag{61}$$

where $\eta = 1$, a strictly positive constant, and $|s_\alpha| = s_\alpha \text{sat}(\frac{s_\alpha}{\beta_\alpha})$. Hence, Equation (60) states that all the system trajectories point towards the sliding surface s_α in a finite time. To be specific, once on the surface, the system trajectories stay on the surface. The conditions are verified by s_α and therefore the inner closed-loop system is guaranteed to be stable.

4 Conclusion

The objective of this thesis is to design the distributed formation control for swarms of UAVs, arranged in tightly and loosely coupled architectures, which addresses the challenges of scalability, collision avoidance, failure recovery, energy efficiency, and control performance. A comprehensive literature review of the general research field of UAVs with a particular emphasis on swarms is presented in Publication I.

The overall system design is based on the formation control of swarms of homogeneous UAVs in a distributed network of leader-follower and leaderless structures in Publications II-IV and Publication V respectively. The leader-follower structure is prone to error propagation and sensitive to the leader's failure. Furthermore, the distributed networks provide user control, system dependability, scalability, and privacy. They behave in a transparent manner, for example, location data is shared and decision-making is divided between the nodes. However, these can become centralised, and can also refer to dispersed networks with a top-down approach. As a result, troubleshooting is easier as system failures, incursions, and crashes may be traced back to specific nodes, making it easier to pinpoint the source of the problem. The model of each node in the swarm formation is based on the nonlinear (Publications II, IV, and V) and linear (Publication III) dynamic models of a quadcopter, i.e. a UAV. Exhibiting the concept of the proposed control designs, this model presents itself as a case study for swarms of UAVs. This addresses Research Question 1.

The overall control scheme of the formation control of swarms of UAVs is divided into high- and low-level control. In the proposed method, an HLC is integrated with an LLC. In the HLC, the setpoints, i.e. desired points of tracking, are generated for the swarms of UAVs considering the complex movement of a hierarchical formation, soft landing, and failure recovery. This addresses Research Question 2. In the LLC, a feedback controller is designed to track the setpoints and stabilise the positions of UAVs for smooth manoeuvre in a swarm formation. This addresses Research Question 3.

Due to the hybrid nature of the whole system architecture (system design and control methods), the dependability of each node in terms of its location gives rise to problems in the adjustment of the controller's design parameters. In other words, deviations of a node might cause significant unwanted changes in the other nodes' locations, especially in cases of leader-follower structures. From the HLC perspective, the main contribution is to propose continuous path planning which can quickly re-

act to events. This procedure is defined as the mapping problem, which describes the best shape of the desired swarm formations. Besides this, from the LLC perspective, the main contribution is to manoeuvre the nodes smoothly. This problem addresses the optimal tracking movement of each node from its initial to final position in a swarm formation. Hence, the overall contribution of this thesis can be outlined as follows:

- This work addresses the problem of a distributed formation control that is based on the dynamics of the overall swarm and the local dynamics of each node via implementing the partial controllers i.e., the top-down, bottom-up approach. The formation complexity of a large system of tightly and loosely coupled swarms of UAVs is reduced. To achieve better scalability, a methodology is proposed in which an HLC is integrated with an LLC so that the swarm performs the setpoint decision-making and an individual node tracks the given trajectory.

- To avoid collisions among nodes, continuous path planning is proposed in the HLC. The hierarchical formation and soft landing are executed using a fixed formation in Publications II and III respectively. The reconfiguration of the formation after a single failed node is implemented using a shortest path algorithm in Publication IV. For multiple failed nodes, the reconfiguration of the formation is implemented using combinatorial algorithms (i.e., distance- and time-optimal algorithms) and the TPS method in Publication V. The objectives of the post-failure reconfiguration are to provide collision avoidance and smooth energy-efficient movement.

- To manoeuvre the nodes smoothly, optimal tracking movement is proposed in the LLC. The tracking of setpoints and stabilisation of each node for smooth manoeuvre is handled by a nonlinear SMC with PD control in Publication II and a linear LQR with integral action in Publications II-V. The control performance of each node is improved by reducing the system's settling time as much as possible without introducing oscillations in the response. The parameters of the controllers are determined through testing of the overall dynamics of the swarm, and convergence towards the setpoints is guaranteed.

4.1 Future Work

All the work in this thesis is based on simulations, and it would be valuable to consider experimental studies on small-scale UAVs. Also, potential challenges are discussed in [3].

There can be various directions in which this work can be extended. For instance, variations of system design can be implemented to achieve scalability such

as (1) Heterogeneous models of UAVs or the hybrid combination of homogeneous and heterogeneous UAVs can be considered. (2) Centralised, decentralised or coupling of centralised/decentralised distributed networks can be studied. (3) Similarly, virtual, behaviour-based or their combination with leader-follower structures can be examined.

In a leader-follower structure, the further the follower(s) node is from its respective leader(s)/sub-leader(s) node, the larger oscillations can be observed in a formation. This effect can be compensated/cancelled using other methods such as model predictive control and reinforcement learning [40; 41; 42]. Another possible extension is to improve the proposed solutions to gain better overall system control performance such as robust stability, collision avoidance, and energy efficiency.

5 Overview of Publications

5.1 Swarms of Unmanned Aerial Vehicles – A Survey

UAVs, in the market, come with diversity in the number of propellers. They can also be grouped based on their size, range, and equipment. The sizes can be either nano, mini, regular, or large while the range can be either very close, close, short, mid, or endurance. In this Publication, a survey-type study on UAVs and swarms of UAVs is presented, with a special focus on quadcopters. The mechanics, functionality, organisation, modelling, applications, and autonomy aspects of such UAVs and their swarms are discussed. In addition, the Publication includes the result of an online survey in order to get a picture of public awareness regarding the use of UAV technology. The participants of this survey were from different countries and associated with several professional fields. The results showed that although a large proportion of the responders were concerned about the privacy and security concerns of swarms of UAVs, on the other hand, it can be quite useful in disaster management, environmental mapping, and search and rescue activities.

5.2 Comparison of Linear and Nonlinear Methods for Distributed Control of a Hierarchical Formation of UAVs

A key problem in cooperative robotics is the maintenance of a geometric configuration during movement. As a solution for this, a multi-layered and distributed control system is proposed for the swarm of UAVs in the formation of hierarchical levels based on the leader-follower structure. The complexity of developing a large system can be reduced in this way. To ensure the tracking performance and response time of the ensemble system, nonlinear and linear control designs are presented; (a) SMC connected with a PD controller and (b) LQR with integral action respectively. The safe travel distance strategy for collision avoidance is introduced and integrated into the control designs for maintaining the hierarchical states in the formation. Both designs provide rapid adoption with respect to their settling time without introducing oscillations for the dynamic flight movement of vehicles in the cases of (1) nominal, (2) plant-model mismatch, and (3) external disturbance inputs. Also, the nominal settling time of the swarm is improved by 44% on average when using the nonlinear

method as compared to the linear method. Furthermore, the proposed methods are fully distributed so that each UAV autonomously performs the feedback laws in order to achieve better modularity and scalability.

5.3 Navigation System for Landing a Swarm of Autonomous Drones on a Movable Surface

The development of a navigation system for the landing of a swarm of UAVs on a movable surface is one of the major challenges in building a fully autonomous platform. Hence, the purpose of this study is to investigate the behaviour of a swarm of ten UAVs under the mission of soft landing on a movable surface that has constant speed with oscillations. This swarm, arranged in a leader-follower hierarchical manner, has distributed control units based on LQR with an integral action method. Furthermore, to prevent UAVs from landing arbitrarily, the leader node takes the feedback of translational coordinates from the movable surface and adjusts its position accordingly. Hence, each follower tracks the leader's trail with offsets, taking collision avoidance into account. The design parameters of controllers are mapped in such a way that the simulations demonstrate the feasibility and great potential of the proposed method.

5.4 Development of a Fault-Tolerant Control System for a Swarm of Drones

One of the important challenges in an autonomous swarm of UAVs is the dependability of the swarm to continue its mission. Engine failure or propeller disintegration poses a significant risk to the operation of each node of the swarm, and if it happens the system should be able to tolerate such malfunction by reconfiguring the swarm and reforming if it is necessary. In this Publication, a fault-tolerant control system for an autonomous leader-follower-based swarm of UAVs is presented. For defining the fault model, the full failure of an engine is considered as an emergency situation, and the controller of each node is facilitated to reconfigure the swarm by imposing a bottom-up reformation to bypass the faulty node, which keeps the formation intact as much as possible. The simulation results show the effectiveness of the proposed method with respect to reliability and robust stability.

5.5 Energy-Efficient Post-Failure Reconfiguration of Swarms of Unmanned Aerial Vehicles

In this Publication, the reconfiguration of swarms of UAVs after simultaneous failures of multiple nodes is considered. The objectives of the post-failure reconfiguration are to provide collision avoidance and smooth energy-efficient movement.

To incorporate such a mechanism, three different failure recovery algorithms are proposed, namely TPS, distance- and time-optimal algorithms. These methods are tested on six swarms, with two variations on failing nodes for each swarm. The simulation results of reconfiguration show that the execution of such algorithms maintains the desired formations with respect to avoiding collisions at run-time. Also, the results show the effectiveness of the proposed methods concerning the distance travelled, kinetic energy, and energy efficiency. As expected, the distance-optimal algorithm gives the shortest movements, and the time-optimal algorithm gives the most energy-efficient movements. The TPS is also found to be energy-efficient and has less computational cost than the other two proposed methods. Despite the suggested heuristics, these are combinatorial in nature and might be difficult to use in practice. Furthermore, the use of the regularisation parameter λ in TPS is also investigated, and it is found that too large values of λ can lead to incorrect locations, including multiple nodes in the same location. In fact, it is found that using $\lambda = 0$ works well in all cases.

List of References

[1] Gaemus Collins, David Twining, and Joshua Wells. Using Vessel-Based Drones to Aid Commercial Fishing Operations. In *OCEANS 2017*, pages 1–5, Aberdeen, UK, 2017.

[2] Małgorzata Polkowska. Technical and Legal Problems of Space Drones. *Zeszyty Naukowe SGSP*, 85:233–249, 2023.

[3] Syed Agha Hassnain Mohsan, Nawaf Qasem Hamood Othman, Yanlong Li, Mohammed H. Alsharif, and Muhammad Asghar Khan. Unmanned Aerial Vehicles (UAVs): Practical Aspects, Applications, Open Challenges, Security Issues, and Future Trends. *Intelligent Service Robotics*, 16:109–137, 2023.

[4] Marianne Harbo Frederiksen and Mette Præst Knudsen. *Drones for Offshore and Maritime Missions: Opportunities and Barriers*. SDU Centre for Integrative Innovation Management, Denmark, 2018.

[5] Christopher S. Tang and Lucas P. Veelenturf. The strategic role of logistics in the industry 4.0 era. *Transportation Research Part E: Logistics and Transportation Review*, 129:1–11, 2019.

[6] Manel Khelifi and Ismail Butun. Swarm Unmanned Aerial Vehicles (SUAVs): A Comprehensive Analysis of Localization, Recent Aspects, and Future Trends. *Journal of Sensors*, 8600674:1–10, 2022.

[7] Ursula K. Verfuss, Ana Sofia Aniceto, Danielle V. Harris, Douglas Gillespie, Sophie Fielding, Guillermo Jiménez, Phil Johnston, Rachael R. Sinclair, Agnar Sivertsen, Stian A. Solbø, Rune Storvold, Martin Biuw, and Roy Wyatt. A Review of Unmanned Vehicles for the Detection and Monitoring of Marine Fauna. *Marine Pollution Bulletin*, 140:17–29, 2019.

[8] Farha Jahan, Weiqing Sun, Quamar Niyaz, and Mansoor Alam. Security Modeling of Autonomous Systems: A Survey. *ACM Computing Surveys*, 52(5, Article 91):1–34, 2019.

[9] Hui-Min Huang. *Autonomy Levels for Unmanned Systems (ALFUS) Framework*, volume I: Terminology version 2.0. National Institute of Standards and Technology, Special Publication 1011-I-2.0, 2008.

[10] Kiattisin Kanjanawanishkul. Formation Control of Mobile Robots: Survey. *UBU Engineering Journal*, 4(1):50–64, 2011.

[11] Bassem Hichri, Abir Gallala, Francesco Giovannini, and Slawomir Kedziora. Mobile Robots Path Planning and Mobile Multirobots Control: A Review. *Robotica, Cambridge University Press*, 40 (12):4257–4270, 2022.

[12] John Thomas and Pam Mantri. Complex Adaptive Blockchain Governance. *MATEC Web of Conferences*, 223(01010):1–23, 2018.

[13] Payam Nourizadeh, Aghil Yousefi-Koma, and Moosa Ayati. Design and Implementation of a Fuzzy Adaptive Controller for Time-Varying Formation Leader-Follower Configuration of Nonholonomic Mobile Robots. *arXiv,cs.RO*, 2205.11174:1–11, 2022.

[14] Paul Wang and Fred Y. Hadaegh. Coordination and Control of Multiple Microspacecraft Moving in Formation. *Journal of the Astronautical Sciences*, 44(3):315–355, 1996.

[15] D. Galzi and Yuri Shtessel. UAV Formations Control Using High Order Sliding Modes. In *2006 American Control Conference*, pages 4249–4254, Minneapolis, MN, USA, 2006.

[16] Ben Yun, Ben M. Chen, Kai Yew Lum, and Tong H. Lee. Design and Implementation of a Leader-Follower Cooperative Control System for Unmanned Helicopters. *Journal of Control Theory and Applications*, 8(1):61–68, 2010.

[17] Omar Mechali, Limei Xu, Xiaomei Xie, and Jamshed Iqbal. Theory and Practice for Autonomous Formation Flight of Quadrotors via Distributed Robust Sliding Mode Control Protocol with Fixed-Time Stability Guarantee. *Control Engineering Practice*, 123(105150):1–26, 2022.

[18] M. Anthony Lewis and Kar-Han Tan. High Precision Formation Control of Mobile Robots Using Virtual Structures. *Autonomous Robots*, 4(4):387–403, 1997.

[19] Tobias Paul, Thomas R. Krogstad, and Jan Tommy Gravdah. Modelling of UAV Formation Flight using 3D Potential Field. *Simulation Modelling Practice and Theory*, 16(9):1453–1462, 2008.

[20] Zhou Chao, Shao-Lei Zhou, Lei Ming, and Wen-Guang Zhang. UAV Formation Flight Based on Nonlinear Model Predictive Control. *Mathematical Problems in Engineering*, 2012(Article ID 261367):1–15, 2012.

[21] Tucker Balch and Ronald C. Arkin. Behavior-Based Formation Control for Multirobot Teams. *IEEE Transactions on Robotics and Automation*, 14(6):926–939, 1998.

[22] Jonathan R. T. Lawton, Randal W. Beard, and Brett J. Young. A Decentralized Approach to Formation Maneuvers. *IEEE Transactions on Robotics and Automation*, 19(6):933–941, 2003.

[23] Derek Bennet and C. R. McInnes. Verifiable Control of a Swarm of Unmanned Aerial Vehicles. *Proceedings of the Institution of Mechanical Engineers, Part G: Journal of Aerospace Engineering*, 223(7):939–953, 2009.

[24] Kwang-Kyo Oh, Myoung-Chul Park, and Hyo-Sung Ahn. A Survey of Multi-Agent Formation Control. *Automatica*, 53:424–440, 2015.

[25] Samir Bouabdallah and Roland Siegwart. Full Control of a Quadrotor. In *2007 IEEE/RSJ International Conference on Intelligent Robots and Systems*, pages 153–158, San Diego, CA, USA, 2007.

[26] Robert Niemiec and Farhan Gandhi. A Comparison Between Quadrotor Flight Configurations. In *42nd Annual European Rotorcraft Forum*, Lille, France, 2016.

[27] Mohammad Fatin Fatihur Rahman, Shurui Fan, Yan Zhang, and Lei Chen. A Comparative Study on Application of Unmanned Aerial Vehicle Systems in Agriculture. *Agriculture*, 11(1):1–26, 2021.

[28] FRANTIŠEK Šolc. Modelling and Control of a Quadrocopter. *Advances in Military Technology*, 5(2):29–38, 2010.

[29] Petr Gabrlik, Vlastimil Kriz, and Ludek Zalud. Reconnaissance Micro UAV System. *Acta Polytechnica CTU Proceedings*, 2:15–21, 2015.

[30] Quan Quan. *Introduction to Multicopter Design and Control*. Springer, Singapore, 2017.

[31] Changcai Yang, Yizhang Liu, Xingyu Jiang, Zejun Zhang, Lifang Wei, Taotao Lai, and Riqing Chen. Non-Rigid Point Set Registration via Adaptive Weighted Objective Function. *IEEE Access*, 6:75947–75960, 2018.

[32] Ping Guo, Wei Hu, Haibing Ren, and Yimin Zhang. PCAOT: A Manhattan Point Cloud Registration Method Towards Large Rotation and Small Overlap. In *2018 IEEE/RSJ International Conference on Intelligent Robots and Systems (IROS)*, pages 7912–7917, Madrid, Spain, 2018.

[33] Andriy Myronenko and Xubo Song. Point Set Registration: Coherent Point Drift. *IEEE Transactions on Pattern Analysis and Machine Intelligence*, 32(12):2262–2275, 2010.

[34] Haili Chui and Anand Rangarajan. A New Algorithm for Non-Rigid Point Matching. In *Proceedings IEEE Conference on Computer Vision and Pattern Recognition. CVPR 2000 (Cat. No.PR00662)*, pages 44–51 vol.2, Hilton Head, SC, USA, 2000.

[35] Michael Safonov and Michael Athans. Gain and Phase Margin for Multiloop LQG Regulators. *IEEE Transactions on Automatic Control*, 22(2):173–179, 1977.

[36] Qasim Ali and Sergio Montenegro. Explicit Model Following Distributed Control Scheme for Formation Flying of Mini UAVs. *IEEE Access*, 4:397–406, 2016.

[37] Catherine Massé, Olivier Gougeon, Duc-Tien Nguyen, and David Saussié. Modeling and Control of a Quadcopter Flying in a Wind Field: A Comparison Between LQR and Structured $\mathscr{H}\infty$ Control Techniques. In *2018 International Conference on Unmanned Aircraft Systems (ICUAS)*, pages 1408–1417, Dallas, TX, USA, 2018.

[38] Diego A. Mercado, Rafael S. Castro, and Rogelio Lozano. Quadrotors Flight Formation Control Using a Leader-Follower Approach. In *2013 European Control Conference (ECC)*, pages 3858–3863, Zurich, Switzerland, 2013.

[39] Jean-Jacques E. Slotine and Weiping Li. *Applied Nonlinear Control*. Englewood Cliffs, N.J: Prentice-Hall, 1991.

[40] Soyeon Koo, Seungkeun Kim, and Jinyoung Suk. Model Predictive Control for UAV Automatic Landing on Moving Carrier Deck with Heave Motion. *IFAC-PapersOnLine, 3rd IFAC Workshop on Multivehicle Systems*, 48(5):59–64, 2015.

[41] Emil Boström and Erik Börjesson. *Autonomous Landing of an Unmanned Aerial Vehicle on an Unmanned Ground Vehicle using Model Predictive Control*. Master of Science Thesis in Electrical Engineering, Department of Electrical Engineering, Linköping University, Linköping, Sweden, 2022.

[42] Fadi AlMahamid and Katarina Grolinger. Autonomous Unmanned Aerial Vehicle Navigation using Reinforcement Learning: A Systematic Review. *Engineering Applications of Artificial Intelligence*, 115(105321):1–20, 2022.

TURUN
YLIOPISTO
UNIVERSITY
OF TURKU

Painosalama, Turku, Finland 2023

ISBN 978-951-29-9412-0 (PRINT)
ISBN 978-951-29-9411-3 (PDF)
ISSN 2736-9390 (PRINT)
ISSN 2736-9684 (ONLINE)